



Renewable fuels from pyrolysis of *Dunaliella tertiolecta*: An alternative approach to biochemical conversions of microalgae



Nejmi Söyler^a, Jillian L. Goldfarb^b, Selim Ceylan^{a,*}, Melek Türker Saçan^c

^a Ondokuz Mayıs University, Chemical Engineering Department, 55139, Samsun, Turkey

^b Boston University, Department of Mechanical Engineering and Division of Materials Science & Engineering, 110 Cummington Mall, Boston, MA 02215, USA

^c Bogazici University, Institute of Environmental Sciences, 34342, İstanbul, Turkey

ARTICLE INFO

Article history:

Received 20 July 2016

Received in revised form

28 November 2016

Accepted 30 November 2016

Available online 4 December 2016

Keywords:

D. tertiolecta

TG-FTIR

Microalgae

Pyrolysis

Biofuel

Activation energy

ABSTRACT

The cultivation of microalgae as a feedstock for renewable fuels is widely touted as a way to sequester CO₂ while negating food versus fuel competition for land. However, the widespread industrial use of microalgae for biofuels has yet to reach a critical stage based on lipid extraction alone. One alternative to the transesterification of microalgae for liquid fuel production is to use thermochemical conversion techniques. In the present work, we demonstrate that *Dunaliella tertiolecta* can be converted to biofuels via pyrolysis at temperatures significantly lower than terrestrial biomasses. The primary gaseous pyrolysis products were CO₂, H₂O, CH₄, alcohols, aldehydes, organic acids and phenols. The iso-conversional distributed activation energy model was used to calculate the kinetic parameters, showing average activation energy of 243.3 kJ/mol, with a peak in activation energy at mass fraction conversions between 0.45 and 0.65. However, the substantial amount of pyrolysis gases evolved at low temperatures (between 280 and 320 °C), suggests that pyrolysis at higher temperatures, and especially to completion, might not be necessary to optimize pyrolytic production of biofuels from microalgae.

© 2016 Elsevier Ltd. All rights reserved.

1. Introduction

The International Energy Agency predicts that global use of biofuels for transportation could grow from 2% in 2011 to 27% by the year 2050, significantly reducing net CO₂ emissions and enhancing energy security [1]. Fulfilling the growing demand for renewable fuels will require a range of solutions to meet the diverse cultivation and processing capabilities across the globe. And while many have jumped on the algal biodiesel bandwagon over the past half century, the high lipid content required for economical production of fuel via transesterification necessitates less-than-optimal algal growth rates, and the high materials and processing costs make all but the largest processes marginally viable [2]. This is not to say that microalgae should be overlooked as a potential fuel precursor; upwards of 70,000 species of microalgae are thought to inhabit earth [3]. Their varied growth cycles and requirements enable cultivation year-round and in many parts of the globe [4]. As compared to terrestrial biomass, microalgae are more efficient in terms of CO₂ fixation and solar energy conversion and they do not

compete for arable land or food [5]. As such, a plethora of recent research explores thermochemical processes such as pyrolysis, gasification and hydrothermal liquefaction for the conversion of microalgae to biofuels [6].

Though combustion of microalgae leads to a higher overall biomass conversion than pyrolysis (which yields considerable solid char), the advantage of thermochemical conversion processes is the potential to produce transportation fuels [7]. However, one of the biggest drawbacks to using thermochemical conversion methods to extract fuels from biomass are the high temperatures required to decompose the solid. As such, marine biomasses such as microalgae may represent a superior feedstock for thermochemical conversion over terrestrial biomasses given their considerably lower decomposition temperatures [8]. *Dunaliella tertiolecta* is an especially strong candidate for biofuel production as it can be cultivated in saltwater, wastewater or brackish water, is highly motile with a high salt tolerance, and is able to withstand a wide range of temperature and light cultivation conditions [9]. Minowa et al. demonstrated a net positive energy gain for the hydrothermal liquefaction of *D. tertiolecta* with oil yields on average of 37 wt% between 250 and 340 °C [10], and Shuping et al. from the same species of 26 wt% at 360 °C [11]. Pyrolysis is another possible route

* Corresponding author.

E-mail address: selim.ceylan@omu.edu.tr (S. Ceylan).

to extract biofuels from microalgae, resulting in liquid fuel yields ranging from 31 to 58% [12,13]. Importantly, Grierson et al. estimated that the energy input for the slow pyrolysis of a series of microalgae at 500 °C is approximately 1 MJ/kg, a requirement easily offset by the combustion of pyrolysis gas produced, which range in heats of combustion from 1.2 to 4.9 MJ/kg [14].

A handful of studies probe the pyrolytic decomposition of microalgae, including *D. tertiolecta*, reporting activation energy values and some bio-oil analyses. However, this is the first study (that the authors could locate) that uses TG-FTIR to analyze real-time changes in decomposition and evolving gas components as a function of temperature. Such information is critically important in terms of designing pyrolysis reactors with appropriate residence times and peak reaction temperatures for the efficient conversion of algal biomass to biofuels [15].

2. Materials & methods

D. tertiolecta is a commercially viable microalgae, currently cultivated for aquaculture food supply and industrial β -carotene production, and has a maximum rate of CO₂ removal of 13.8 mg L⁻¹ min⁻¹ [16]. This microalgae is green with radial symmetry, whose cell dimensions range from 8 to 15 μ m long to 5–6 μ m wide and flagella are approximately 1.5 times its cell length. Though its optimal salinity is approximately 3 w/v% NaCl, like all algae of the genus *Dunaliella* it is adaptable to a wide range of salinities, and can tolerate heavy metals and pesticides [17].

2.1. Microalgae cultivation and characterization

D. tertiolecta was obtained from the Ecotoxicology and Chemometrics Laboratory at the Institute of Environmental Sciences, Bogazici University, Turkey. The inoculum was prepared with algae harvested from 4 to 5 day-old cultures in the exponential growth phase. It was cultured in filtered (GF/C glass microfiber Whatman filters) natural seawater,¹ enriched with modified f/2 medium [19]. The pH of the medium was 8.2 \pm 0.1. Each milliliter of inoculum contained approximately 10⁴ cells. 100 mL of test medium with algae was dispensed into sterile 500 mL borosilicate Erlenmeyer flasks and kept in a temperature-controlled growth chamber (18 \pm 0.5 °C). Continuous illumination (30 mmol photons m⁻²s⁻¹ at the level of test solutions) was provided from a rack of cool-white fluorescent tubes, arranged horizontally above a light-reflecting platform on which the test vessels were located. Cultures were undisturbed for 10 days; at the beginning of stationary phase the biomass was harvested using centrifugation at 4000 RPM (SELECTA) for 20 min and dried in an oven at 60 °C for several days.

The *D. tertiolecta* samples were characterized via proximate and ultimate analysis. Proximate analysis was determined on a thermogravimetric analyzer (Shimadzu). The samples were heated to constant mass at 105 °C to remove residual moisture. Volatiles were determined as the mass loss up to 950 °C in nitrogen, with ash content determined as total sample left after complete oxidation, and fixed carbon by difference. Ultimate analysis was performed in a Leco CHN-932 (Leco, Germany). The higher heating value of *D. tertiolecta* was determined using an IKA C 200 oxygen bomb calorimeter (IKA, China). The possible chemical functional groups

present in the *D. tertiolecta* biomass were investigated with FTIR (Perkin Elmer, Spectrum-Two, USA) in the range of 4000–650 cm⁻¹ wavelength using 32 scans and 4 cm⁻¹ resolution to background spectra recorded in the air.

2.2. Thermochemical conversion of microalgae

Thermogravimetric analysis (TGA) is widely employed to probe the thermal conversion of biomass to biofuels, shedding light on reaction kinetics and activation energies required to initiate devolatilization at various stages. TGA enables measurement of the amount and rate of decomposition as a function of temperature and time in a controlled atmosphere. Such data are useful for the operation and design of pyrolysis systems [20]. A Shimadzu TGA was used to evaluate the pyrolytic behavior of *D. tertiolecta* under an inert N₂ atmosphere with a gas flow rate of 80 mL min⁻¹ using sintered α -alumina as a reference material. Approximately 10 mg of sample was placed directly into a platinum crucible. A series of three samples were heated from room temperature to 110 °C and held constant for 20 min to remove moisture. Then, the temperature was increased at 5, 10 or 20 °C min⁻¹ to 800 °C, at which point the mass was constant.

2.2.1. Analysis of gaseous products via FTIR

To monitor the gaseous products released during pyrolysis of *D. tertiolecta*, a Fourier-transform infrared spectrometer (Bruker Tensor 27 FTIR) was coupled to the TGA during a 20 °C min⁻¹ experiment. The flow cell connecting the TG and FTIR was heated to 200 °C to prevent condensation of the produced gas on the cell wall, and to minimize secondary reactions. The scan range was 4000–650 cm⁻¹ at a resolution of 1 cm⁻¹. Wavelengths associated with various functional groups used for spectrum analysis are given in Table 1. Such information, when coupled with kinetic parameters, is critically important to the design of large-scale pyrolysis applications [4,21].

2.2.2. Determination of kinetic parameters

Various mathematic models are applied for the determination of kinetic parameters using TGA data from biomass pyrolysis. In particular, the Distributed Activation Energy Model (DAEM) is widely used to determine biomass kinetics [22,23] and specifically of micro and macroalgae species [20,24,25]. The DAEM (and its application here) conforms to the ICTAC Kinetics Committee's recommendation of using an isoconversional approach to limit the impact of potential heat and mass transfer limitations on overall kinetic parameters [26]. The DAEM assumes that pyrolysis proceeds via concurrent first-order parallel chemical reactions with different rates that can be modeled as an overall irreversible first-order reaction. Briefly, the DAEM is expressed as:

$$1 - V/V^* = \int_0^{\infty} \Phi(E, T) f(E) dE \quad (1)$$

where V/V^* represents the mass fraction degree of conversion, and $f(E)$ is a Gaussian distribution function of the activation energy.² $\Phi(E, T)$ often represents an Arrhenius expression (hence the assumption of parallel first order reactions) and is written as:

² While functions other than a normal (Gaussian) distribution can be used to describe biomass pyrolysis, including Weibull, Gamma, and Maxwell-Boltzmann distributions [27–29]. In this case, as in many others of solid biomass pyrolysis, a normal distribution well represented the data.

¹ Seawater was taken from the Sea of Marmara, near the coast of Samatya, Istanbul, and was stored at -24 °C in a plastic container after filtration. Natural seawater characterization was made based on standard procedures (APHA-AWWA-WEF, 1998). In addition, the concentration of environmentally significant heavy metals (Al, Pb, Zn, Cd, Cu, Cr, Ni, Co) in the seawater was measured using ICP-OES (Perkin Elmer Optima 2100 DV), the results of which are available in a previous study [18].

Table 1
FTIR spectrum assignments used for analysis of *D. tertiolecta*.

Wave number (cm ⁻¹)	Functional group	Attributable components
<i>Functional groups assigned to peaks on solid D. tertiolecta surface</i>		
~3250	O–H	Water
~2920	C–H	Methylene groups of lipids
~1750	C=O	Ester functional groups primarily from lipids and fatty acids
~1650	N–H	Mainly associated with proteins; assigned as the amide I band. May also contain contributions from C–C stretches of olefinic and aromatic compounds
~1550	C–H and N–H	Associated with proteins
~1450	C–H	CH ₃ and CH ₂ of proteins
~1250	C–O	Ester functional groups primarily from lipids and fatty acids
~900	C–O–C	Polysaccharides
<i>Functional groups assigned to devolatilized gases from D. tertiolecta pyrolysis</i>		
4000–3400	O–H	H ₂ O
3000–2700	C–H	CH ₄
2400–2250	C=O	CO ₂
2250–2000	C–O	CO
1900–1650	C=O	Aldehydes, ketones, acids
1690–1450	C=C	Aromatics
1475–1000	C–O, C–C	Alkanes, alcohols, phenols, ethers, lipids
<i>Fingerprint region of 1475–1000</i>		
1460–1365	C–H, C–C	Alkanes
1300–1200	C–O	Phenols
1300–1050	C–O	Lipids
1275–1060	C–O	Ethers
1200–1000	C–O	Alcohols
586–726	C=O	CO ₂

$$\Phi(E, T) = \exp\left(-\frac{k}{\beta} \int_0^T e^{-E/RT} dT\right) \quad (2)$$

where k is the pre-exponential factor, T the absolute temperature, R the Universal gas constant, and β represents the heating rate. Here we employ Miura and Maki's [30] simplification to the DAEM (essentially assuming $\Phi(E, T) = 1$) such that:

$$\ln\left(\frac{\beta}{T^2}\right) = \ln\left(\frac{kR}{E}\right) + 0.6075 - \frac{E}{RT} \quad (3)$$

Equation (3) enables one to obtain kinetic parameters for the thermal decomposition under both inert and oxidative environments. A plot of $\ln(\beta/T^2)$ versus $1/T$ at each fractional conversion is a straight line such that the activation energy and pre-exponential factor are directly calculated from the slope and intercept, respectively.

3. Results & discussion

Though the chemical composition of microalgae varies depending on species and cultivation conditions, they tend to be higher in lipid and sugar content and slightly lower in ash content than their macroalgal counterparts. In this sense, microalgae may represent a more efficient biomass source than macroalgae given heat and mass transfer limitations in high ash biomasses, which lead to agglomeration, slagging and fouling in boilers [31,32].

3.1. Analysis of raw biomass

In this study, we followed OECD Guideline 201 [33] for algal cultivation; the initial cell density was 1×10^4 cells mL⁻¹, with a final

cell density (after 10 days of batch cultivation) was 2×10^6 cells mL⁻¹. Thus, the algal population increased by at least a factor of 16, corresponding to a specific growth rate of 0.92 d⁻¹. The algal biomass was characterized by proximate and ultimate analyses, the results of which are provided in Table 2. *D. tertiolecta* exhibited a carbon content of 42.65% and a hydrogen content of 6.11%. The nitrogen content was 1.14%, attributed to the chlorophyll, nucleic acids, and glucosamides along with cell wall materials of microalgae [34]. The nitrogen ratio of *D. tertiolecta* is relatively low compared to that of other microalgae species such as *Nannochloropsis* (3.14%), *Spirulina* (3.58%), and *C. vulgaris* (9.48%) [4,22]. In biomass pyrolysis, nitrogen leads to the formation of hazardous NO_x compounds. Thus, the lower N content of *D. tertiolecta* is favorable in terms of atmospheric emissions. The ash content of *D. tertiolecta* was 14.21%, less than the 25.7 wt% of *Lyngbyasp* measured by Maddi et al. [35]. The ash content results from microalgae's constant exposure to minerals during cultivation. The heat of combustion (HHV) of *D. tertiolecta* was measured as 16.22 MJ kg⁻¹; like terrestrial biomasses, literature values for the HHV of various microalgae range widely, from 14.24 MJ kg⁻¹ to 21.14 for *D. tertiolecta* [11,36] to 21.88 MJ kg⁻¹ for *Chlorella vulgaris* [37].

D. tertiolecta has been reported to contain approximately 29 wt% proteins, 11 wt% lipids and 14 wt% sugars [38], though others suggest these values may be lower [39]. Analysis of surface functional groups of solid *D. tertiolecta* was performed using FTIR according to the spectral analysis in Table 1. A large peak at 3250 cm⁻¹ was attributed to the stretching of primarily –OH groups. The stretching associated with a peak at 2920 cm⁻¹ of C–H is suggestive of lipid's methylene group. The strong, intense peak at 1750 cm⁻¹ likely corresponds to C=O amide stretching from proteins present in *D. tertiolecta*. The bands observed at 1650 and 1550 cm⁻¹ are associated mainly with the protein content of *D. tertiolecta*. A peak spanning 1450 cm⁻¹ is likely indicative of C–H bending vibration in methyl and methylene groups. A peak at 1250 cm⁻¹ is thought to be the C–O stretching of organic acids. An absorbance peak at 900 cm⁻¹ is likely vibrational stretching of C–O–C from polysaccharides.

3.2. Thermochemical conversion

To determine the kinetics and products of pyrolysis of *D. tertiolecta*, we employed TGA coupled with FTIR. Data were analyzed using the Distributed Activation Energy Model.

3.2.1. Thermal analysis and kinetic parameters

The thermal profiles for the pyrolysis of *D. tertiolecta* at 5, 10, and 20 °C min⁻¹ show a strong dependence of devolatilization rate on heating rate; this is of course well documented in the literature for both pyrolytic and oxidative decompositions of microalgae [24,40]

Table 2
Characterization of raw *D. tertiolecta*.

<i>Proximate analysis (wt %)</i>	
Moisture	8.15
Volatile matter ^{db}	61.82
Fixed carbon ^{db,a}	22.71
Ash ^{db}	15.47
<i>Ultimate analysis (wt%)</i>	
C	42.65
H	6.11
N	1.14
O ^a	50.10
Higher heating value (MJ kg ⁻¹)	16.22

db = dry basis.

a = by difference.

and is the motivating factor behind using isoconversional kinetic analyses [26]. As shown in Fig. 1, as the heating rate increases, the residence time of the sample at each temperature is decreased, and as a result the corresponding initial and final decomposition temperatures are delayed. Also in Fig. 1 are the derivative thermogravimetric (DTG) curves, showing a two-stage pyrolysis process. In first stage, at temperatures below 120 °C, mass loss is attributed predominantly to moisture removal. In the second stage we see the devolatilization of the biomass over a large temperature range of ~220–450 °C as the carbohydrates, lignin, lipids and proteins undergo a suite of decomposition mechanisms, including depolymerization, decarboxylation and cracking of primarily carbohydrates, lignins, lipids and proteins. The DTG curves indicate the highest rate of decomposition occurs between 310 and 350 °C. The shoulder observed at the second stage of the DTG curves is likely due to the presence of lipids and proteins in the microalgae, as reported by Kebelmann et al. [31] and Bui et al. [41].

To study the reaction kinetics of *D. tertiolecta* pyrolysis, we used the Distributed Activation Energy Model to determine the activation energy as a function of mass fraction conversion. The Arrhenius plot according to Equation (3) is shown in Fig. 2. The correlation coefficients (R^2) at each conversion value was greater than 0.99, indicating suitable applicability of the DAEM [26]; values at each conversion are given in Table 3. Overall, the activation energies of pyrolysis of various microalgae species in the literature range from 50 to 334 kJ mol⁻¹. As shown in Fig. 3, the activation energy of pyrolysis increases as the mass fraction converted increases, peaking between 0.45 and 0.65, with conversion above this peak having statistically significantly higher activation energies than those below 0.40. The activation energy measured here are on the higher end of activation energies calculated with the DAEM for the pyrolysis of different microalgae species across the literature, as detailed in Table 4. Shuping et al. [42] measure the activation energy of pyrolysis of *D. tertiolecta* using different isoconversional models (Kissinger, Flynn and Wall) and find a lower activation energy (145.7 kJ mol⁻¹), though they also observe a peak in activation energy between 0.40 and 0.60 fractional conversions. However, as detailed in the Supplemental Information, the activation energy calculated using five other isoconversional models (Friedman, Vyozkin, Starink, Flynn-Wall-Ozawa and Kissinger-Akahira-Sunose) render the same activation energies as the DAEM, suggesting that this is not a “model fit” discrepancy, but rather a potential difference in starting sample or experimental technique.

Further potential differences between the present study and that by Shuping et al. include their use of heating rates up to

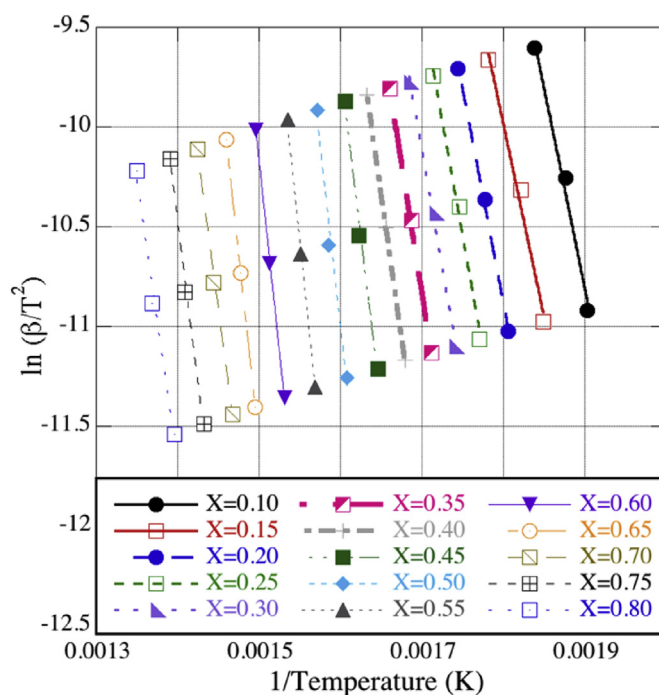


Fig. 2. DAEM plot for *D. tertiolecta* pyrolysis.

40 °C min⁻¹; for future work we propose exploring whether or not the DAEM as applied to microalgae is more susceptible to employing various heating rate ranges than say for terrestrial biomasses. In addition, the *D. tertiolecta* used by Shuping et al. was obtained as a powder by an industrial supplier, presumably it was lyophilized to make it a powder, whereas the algae used here was grown and harvested via centrifugation followed by mild oven drying at 60 °C. It is possible that the freeze-drying process promoting weakening of the biomass structures, decreasing the activation energy required for pyrolysis. The two algae samples vary in proximate and ultimate analyses; the algae used here had higher carbon and hydrogen content and lower oxygen content. The algae used in the Shuping et al. study had a 12.2% lower gross heating value (14.24 MJ/kg versus 16.22 MJ/kg used here) and lower ash content (12.5% lower). The Shuping et al. algae samples therefore have a higher fraction of reactive carbon species, but carbonaceous bonds with weaker energies; a lower ash content would imply a higher heating value (more material available for combustion), but

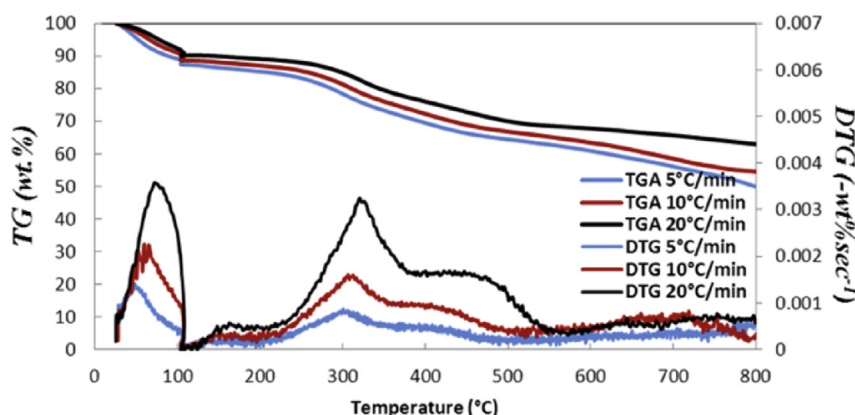
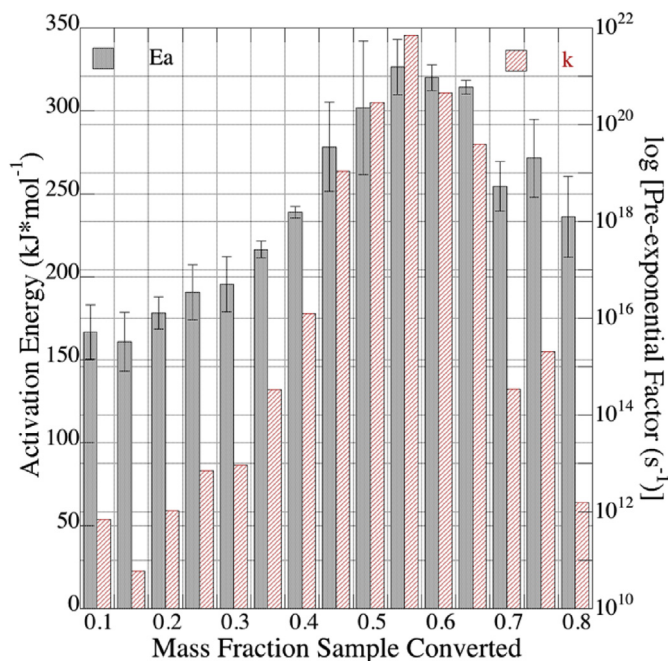


Fig. 1. Mass loss and derivative thermogravimetric curves of *D. tertiolecta* pyrolysis.

Table 3Activation energy of pyrolysis of *D. tertiolecta* at each mass fraction converted as calculated by the DAEM; error indicates \pm one standard deviation.

Weight fraction converted	Activation energy (kJ mol ⁻¹)	Pre-exponential factor	R ²
0.10	166.6 \pm 16.4	7.00E+11 \pm 4.00E+01	0.9904
0.15	160.8 \pm 17.7	6.00E+10 \pm 4.83E+01	0.9880
0.20	178.1 \pm 9.8	1.06E+12 \pm 8.03E+00	0.9970
0.25	190.6 \pm 16.6	6.93E+12 \pm 3.25E+01	0.9925
0.30	195.5 \pm 16.6	9.25E+12 \pm 3.06E+01	0.9928
0.35	216.5 \pm 4.9	3.33E+14 \pm 2.72E+00	0.9995
0.40	238.8 \pm 3.5	1.26E+16 \pm 1.99E+00	0.9998
0.45	278.3 \pm 26.9	1.10E+19 \pm 1.92E+02	0.9907
0.50	301.9 \pm 40.2	2.82E+20 \pm 2.17E+03	0.9826
0.55	326.5 \pm 16.5	6.93E+21 \pm 2.19E+01	0.9974
0.60	320.0 \pm 7.7	4.56E+20 \pm 4.03E+00	0.9994
0.65	314.3 \pm 4.3	3.92E+19 \pm 2.15E+00	0.9998
0.70	254.5 \pm 14.9	3.43E+14 \pm 1.33E+01	0.9966
0.75	271.6 \pm 23.4	2.05E+15 \pm 5.34E+01	0.9926
0.80	236.1 \pm 24.2	1.55E+12 \pm 5.46E+01	0.9896
Average	243.3 \pm 57.45	5.14E+20 \pm 1.78E+21	

**Fig. 3.** Pyrolysis activation energy and pre-exponential factor of *D. tertiolecta* as a function of mass fraction converted (error bars indicate \pm one standard deviation).

instead the carbon bonds present in the Shuping et al. sample may be weaker than those in the current sample, leading to the higher heating value and activation energy observed herein.

Using a simplified DAEM procedure reported by Soria-Verdugo et al. [43], we “predict” the devolatilization curves to further gauge the applicability of the DAEM using Equation (4):

$$T = \frac{-\frac{E}{R}m}{\ln(\beta) - (n + 0.6075) - \ln\left(\frac{kR}{E}\right)} \quad (4)$$

The constants m and n are determined from the plot of $\ln(1/T^2)$ versus $1/T$ at various heating rates according to the linearized form:

$$\ln\left(\frac{1}{T^2}\right) = \frac{m}{T} + n \quad (5)$$

A sample plot of Equation (5) fit to pyrolysis data is given in Fig. S2 of the Supplemental Information. Using the m and n values

Table 4

Average activation energies for various microalgae species from previous studies and this work.

Microalgae	E (kJ*mol ⁻¹)	Reference
<i>Asparagus schoberioides kunth</i>	214.91	[49]
<i>Chlorella pyrenoidosa</i>	143	[22]
<i>Chlorella sorokiniana</i>	78	[25]
<i>Chlorococcum humicola</i>	190	[48]
<i>Dunaliella tertiolecta</i>	145.6	[42]
<i>Dunaliella tertiolecta</i>	243	This study
<i>Enteromorpha clathrata (fixed)</i>	237.5	[49]
<i>Enteromorpha clathrata (floating)</i>	165.32	[49]
<i>Enteromorpha prolifera</i>	228	[50]
<i>Hydrilla verticillata</i>	178	[22]
<i>Monoraphidium 3s35</i>	130	[25]
<i>Nannochloropsis oculata</i>	152	[24]
<i>Tetraselmis sp.</i>	175	[24]
<i>Thallus Laminariae</i>	215.96	[49]
<i>Ulva lactuca L.</i>	192.26	[49]
<i>Undaria pinnatifida (Harv.)</i>	205.6	[49]
<i>Zosterae Marinae L.</i>	50.29	[49]

determined, we simulated the temperature as a function of mass loss and found good agreement with the data, as demonstrated in Fig. 4, for the 10 °C min⁻¹ pyrolysis. Overall, it appears as though Soria-Verdugo et al.’s simplification is a reasonable predictor for the devolatilization of the complex, heterogeneous pyrolysis reactors of *D. tertiolecta*.

Finally, Fig. 3 also plots the pre-exponential factor as a function of mass fraction sample converted; it ranges from 6.00*10¹⁰ to 6.93*10²¹, peaking between 0.45 and 0.65 conversion fractions. We note that the pre-exponential factor decreases more sharply above $V/V^* = 0.70$ than does activation energy. The pre-exponential factor is a function of the collision frequency of molecules during a reaction, and is therefore dependent on both the number and type of molecules present in a given volume. Further, according to Collision Theory, k is only mildly dependent on the reaction temperature [44]. This would suggest that as the concentration of potential reactants decreases – i.e. as fractional conversion increases – that k would also decrease. However, as has been noted for other solid fuel pyrolysis, there is often a peak in k and then a drop as pyrolysis proceeds that does not necessarily follow the trend for activation energy [45]. This behavior can be understood through Fig. 5, which shows a TG curve for 20 °C min⁻¹ pyrolysis plotted with the heat flow required to achieve these temperatures and mass loss. As temperature increases, the mass loss rate slows as the heat required to devolatilize the sample increases. In other words, as the sample

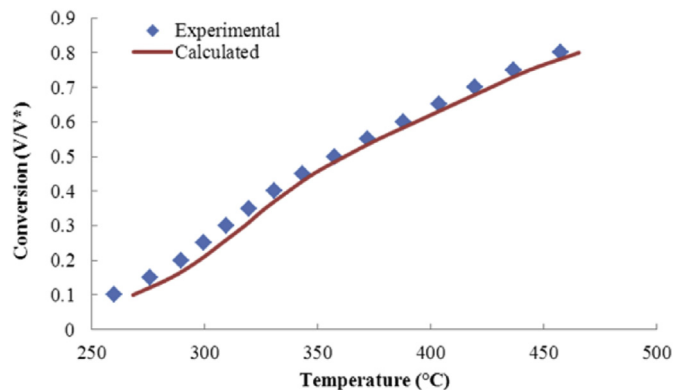


Fig. 4. Calculated (via Gaussian distribution assumption of DAEM) versus experimental data obtained for pyrolysis of *D. tertiolecta* at $10\text{ }^{\circ}\text{C min}^{-1}$.

is nearing exhaustion, the activation energy required to initiate continuing pyrolysis reactions increases; there is less mass and therefore fewer reactants available, and thus the pre-exponential factor decreases. Also in Fig. 5 is the first look at evolved gas analysis, showing distinct peak devolatilized compound regions at the beginning and end of pyrolysis.

3.2.2. TG-FTIR analysis

As we analyze the evolving gases from pyrolysis, we keep the information from Figs. 3 and 5 in mind. Though it is often desirable to “maximize” pyrolytic conversion to convert all carbon present to fuels, it might well be more efficient in terms of energy requirements and product yields to constrain conversions below say 50 wt%. Volatile compounds formed during the pyrolysis of *D. tertiolecta* were analyzed in real time by FTIR coupled with a TGA. Fig. 6 presents the IR spectrum taken at a range of decomposition stages as observed in the DTG curve at $20\text{ }^{\circ}\text{C min}^{-1}$. We choose to use $80\text{ }^{\circ}\text{C}$ as it is below the temperature where we expect to find

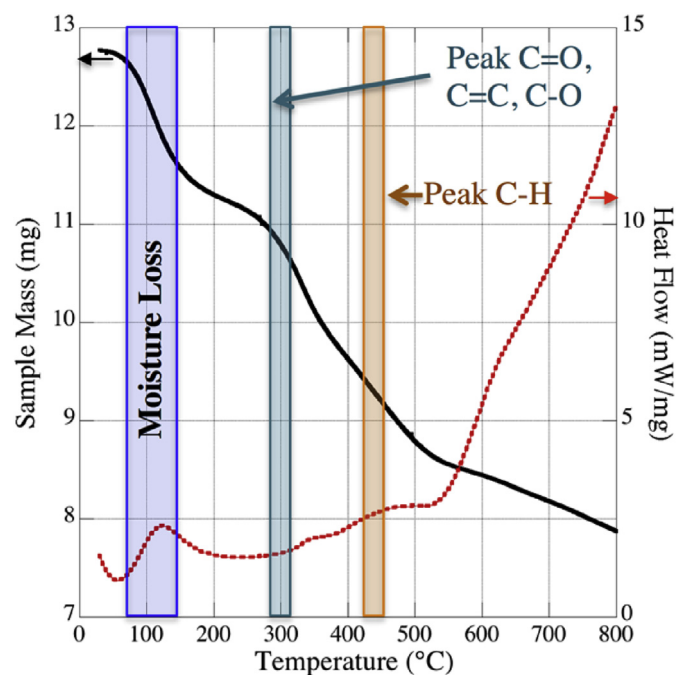


Fig. 5. TG and required heat flow curves showing primary gas evolution regions at $20\text{ }^{\circ}\text{C/min}$ heating rate.

devolatilization of organics, $220\text{ }^{\circ}\text{C}$ as it was the approximate beginning of devolatilization, and $420\text{ }^{\circ}\text{C}$ as the final temperature of observation as the total mass loss and rate drops significantly after this point. The spectrum at $320\text{ }^{\circ}\text{C}$ represents the peak DTG temperature, and spectrum taken at 280 and $380\text{ }^{\circ}\text{C}$ represent the midpoint between onset and peak and a change in slope of the DTG curves, respectively. A 3D plot of continuous nonisothermal spectral data, as well as additional plots highlighting various IR regions, are available in Fig. S3 of the Supplemental Information.

The assigned peaks correspond to the functional groups named in the literature, and are detailed in Table 1. As expected, there were no significant pyrolysis gas peaks noted for the $80\text{ }^{\circ}\text{C}$ spectrum, confirming that mass loss is attributable primarily to water loss at this stage (characteristic signals of water taken to be between 3750 and 3500 cm^{-1}). At $320\text{ }^{\circ}\text{C}$, (peak DTG) the most intense peaks were observed between 2450 and 2250 cm^{-1} . These are ascribed to the C=O stretching of CO_2 . As seen in Fig. 6, though the mass loss rate is highest at this temperature, the FTIR signal intensity in this range is comparable to the $280\text{ }^{\circ}\text{C}$ and $320\text{ }^{\circ}\text{C}$ samples, though almost 50% stronger than that for the $420\text{ }^{\circ}\text{C}$ sample, suggesting that CO_2 -forming compounds are depleted within the peak of the DTG curve.

The intensities of the characteristic peaks of CH_4 associated with C–H stretching between 3000 and 2750 cm^{-1} are virtually indistinguishable for the 280 , 320 , 380 and $420\text{ }^{\circ}\text{C}$ data, though the $220\text{ }^{\circ}\text{C}$ spectrum shows considerably lower absorbance (highlighted in Fig. S3 of the Supplemental Information.) The asymmetrical C–H stretching around $\sim 2950\text{--}3000\text{ cm}^{-1}$ suggests that the methylene group evolution increases as temperature increases, peaking for the $420\text{ }^{\circ}\text{C}$ data.

The absorbance bands between 1900 and 1600 cm^{-1} (highlighted in Fig. 6b) with peaks at approximately 1750 cm^{-1} correspond to the C=O carbonyl stretching of carboxylic acid, ketones, or aldehyde groups. This is again highest for the $280\text{ }^{\circ}\text{C}$ data, followed by the $320\text{ }^{\circ}\text{C}$, though with little evidence of devolution at $220\text{ }^{\circ}\text{C}$. Such carbonyl and carbocyclic compounds are derived from lipid and proteins, and thus we can infer that the initial degradation at $220\text{ }^{\circ}\text{C}$ is likely pyrolysis of the cell wall, whereas devolution of the algal cells is initiated above this temperature. A relatively large peak at 1250 cm^{-1} lies in the fingerprint region of C–O stretching, indicating the presence of phenols or lipids, and again shows the strongest intensity for 280 and $320\text{ }^{\circ}\text{C}$ samples, with little signal for the 80 and $220\text{ }^{\circ}\text{C}$ spectra. Peaks at 1576 cm^{-1} (C=C stretching vibrations) suggest the presence of alkenes and/or aromatics, and are again highest for the 280 and $320\text{ }^{\circ}\text{C}$ samples.

Our FTIR analysis of the data agrees well with other methods employed in the literature to study pyrolysis products of *D. tertiolecta* and other microalgae. Grierson et al. use gas chromatography to study the pyrolysis *D. tertiolecta* at a rate of $10\text{ }^{\circ}\text{C min}^{-1}$, and find a peak CO_2 evolution around $280\text{ }^{\circ}\text{C}$, and a peak for CH_4 at approximately $450\text{ }^{\circ}\text{C}$ [14]. Such peak temperatures are somewhat microalgae-specific, though various species do fall within similar ranges. For example, the peak CO_2 and CH_4 evolution from *Nannochloropsis gaditana* pyrolysis occurs at approximately $350\text{ }^{\circ}\text{C}$, with ethyl and amine groups detected at temperatures above $300\text{ }^{\circ}\text{C}$ [46].

3.3. Pyrolysis of microalgae *D. tertiolecta*

The combined TG-FTIR analysis of the pyrolysis of this microalgae species provides key insight into the feasibility of extracting biofuels from microalgae via pyrolysis. That is, it may be possible to reduce the energy necessary for pyrolysis by maintaining lower temperatures in the reactor. Though data suggest that pyrolysis temperature must be beyond the “onset” of pyrolysis ($\sim 220\text{ }^{\circ}\text{C}$), it is not clear that temperatures must even exceed $300\text{--}380\text{ }^{\circ}\text{C}$ to yield

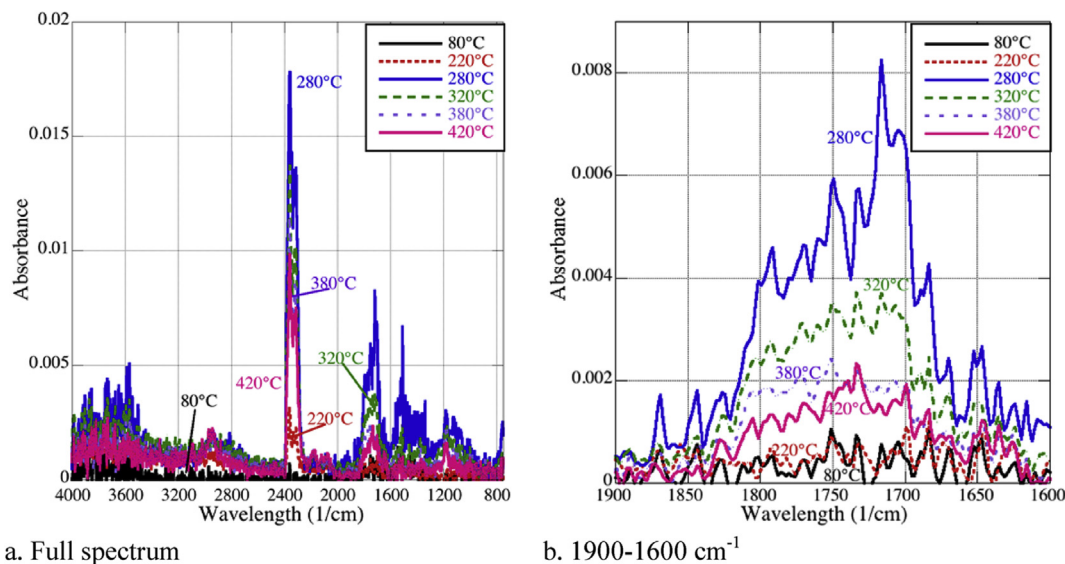


Fig. 6. Selected FTIR data for $20\text{ }^{\circ}\text{C min}^{-1}$ pyrolysis of *D. tertiolecta* at 80, 220, 280, 320, 380 and $420\text{ }^{\circ}\text{C}$ (3D plot and additional “snapshots” available in Supplemental Information).

sufficient amounts of biofuels. This is compared to terrestrial biomasses, which are pyrolyzed at temperatures exceeding $550\text{ }^{\circ}\text{C}$ to render fuels in significant quantities.

Interestingly, *D. tertiolecta* has been found to evolve the least CO_2 of several microalgal species (10% of pyrolysis gases versus 18% for *C. vulgaris*) and the highest CH_4 , with a calorific value of combustible biogas of 2.4 MJ/kg obtained at $500\text{ }^{\circ}\text{C}$ [14]. Furthermore, given the absence of strong amine functional group signals, the lower nitrogen content of *D. tertiolecta* as opposed to other microalgal species may overcome the modestly higher activation energy required for pyrolysis in terms of environmental benefits of reduced NO_x formation.

Kim et al. note the possibility of an integrated biorefinery for the production of biodiesel and pyrolysis fuels, whereby *D. tertiolecta* residual biomass, obtained post-lipid and carbohydrate extraction, could be pyrolyzed to yield a residue bio-oil [47]. Likewise, Francavilla demonstrated the ability to pyrolyze the residue of *D. tertiolecta* following lipid extraction, resulting in up to 45 wt% oil yields [36]. The yield of such bio-oil is likely lower in this integrated concept than for pyrolysis alone (given an overall material balance), but the concept would clearly valorize the biodiesel waste stream. It is recommended that further study on residual algal biomass be conducted in a similar vein to that presented here to identify peak product distribution temperatures to design the most efficient reuse scenario. Others suggest the possibility of co-firing algae with coal to increase reactivity at lower temperatures while using existing infrastructure [48]. In addition, a life cycle analysis on various incarnations of a microalgal biorefinery would shed light on pros and cons of using only pyrolysis versus pyrolysis of residual microalgae, or the feasibility of co-pyrolysis with coal, to produce liquid fuels to meet the IEA's goal of 27% biofuels for the transportation section by 2050 [1].

4. Conclusions

The present study probes the kinetic behavior and evolution of gaseous products for the pyrolysis of *D. tertiolecta*, a marine microalgal species. Thermogravimetric analysis shows that pyrolysis is initiated around $220\text{ }^{\circ}\text{C}$, but simultaneous FTIR analysis suggests that this is only the onset of cell wall decomposition. Rather, devolatilization of the cell (as noted through common lipid

and protein pyrolysis products) begins in earnest around $280\text{ }^{\circ}\text{C}$. Kinetic parameters were calculated using the Distributed Activation Energy Model and used to simulate the pyrolysis process; calculated curves showed good agreement with experimental data. The mean activation energy of *D. tertiolecta* was determined to be 243 kJ mol^{-1} , which is higher than many *Chlorella* algae, and similar to those from the *Enteromorpha* and *Undaria* genera. However, a lower nitrogen content of *D. tertiolecta*, and lower CO_2 yield as compared to other microalgae, are key environmental considerations in the selection of microalgal feedstocks for biofuel production from pyrolysis.

Acknowledgements

The authors thank Gulcin Tugcu for cultivating *D. tertiolecta*. This study was supported by Ondokuz Mayıs University with a project number of PYO.MUH.1904.15.012 and TÜBİTAK with a project number of 214M153.

Appendix A. Supplementary data

Supplementary data related to this article can be found at <http://dx.doi.org/10.1016/j.energy.2016.11.146>.

References

- [1] International Energy Agency (IEA). Technology roadmap: biofuels for transport. 2011. www.iea.org [Accessed 8 July 2016].
- [2] Petkov G, Ivanova A, Iliiev I, Vaseva I. A critical look at the microalgae biodiesel. *Eur J Lipid Sci Technol* 2012;114(2):103–11.
- [3] Guiry MD. How many species of algae are there? *J Phycol* 2012;48(5):1057–63.
- [4] Peng X, Ma X, Lin Y, Guo Z, Hu S, Ning X. Co-pyrolysis between microalgae and textile dyeing sludge by TG–FTIR: kinetics and products. *Energy Convers Manag* 2015;100:391–402.
- [5] Clarens AF, Resurreccion EP, White MA, Colosi LM. Environmental life cycle comparison of algae to other bioenergy feedstocks. *Environ Sci Technol* 2010;44(5):1813–9.
- [6] Marcilla A, Catalá L, García-Quesada JC, Valdés FJ, Hernández MR. A review of thermochemical conversion of microalgae. *Renew Sustain Energy Rev* 2013;27:11–9.
- [7] Agrawal A, Chakraborty S. A kinetic study of pyrolysis and combustion of microalgae *Chlorella vulgaris* using thermo-gravimetric analysis. *Bioresour Technol* 2013;128:72–80.
- [8] López-González D, Fernandez-Lopez M, Valverde J, Sanchez-Silva L. Kinetic analysis and thermal characterization of the microalgae combustion process

- by thermal analysis coupled to mass spectrometry. *Appl Energy* 2014;114:227–37.
- [9] Tang H, Abunasser N, Garcia MED, Chen M, Ng KYS, Salley SO. Potential of microalgae oil from *Dunaliella tertiolecta* as a feedstock for biodiesel. *Appl Energy* 2011;88:3324–30.
 - [10] Minowa T, Yokoyama S-Y, Kishimoto M, Okakura. Oil production from algal cells if *Dunaliella tertiolecta* by direct thermochemical liquefaction. *Fuel* 1995;74:1735–8.
 - [11] Shuping Z, Yulong W, Mingde Y, Kaleem I, Chun L, Tong J. Production and characterization of bio-oil from hydrothermal liquefaction of microalgae *Dunaliella tertiolecta* cake. *Energy* 2010;35(12):5406–11.
 - [12] Pan P, Hu C, Yang W, Li Y, Dong L, Zhu L, et al. The direct pyrolysis and catalytic pyrolysis of *Nannochloropsis* sp. residue for renewable bio-oils. *Bioresour Technol* 2010;101(12):4593–9.
 - [13] Miao X, Wu Q. High yield bio-oil production from fast pyrolysis by metabolic controlling of *Chlorella protothecoides*. *J Biotechnol* 2004;110(1):85–93.
 - [14] Grierson S, Strezov V, Ellem G, Mcgregor R, Herbertson J. Thermal characterisation of microalgae under slow pyrolysis conditions. *J Anal Appl Pyrolysis* 2009;85(1):118–23.
 - [15] Raheem A, Azlina WW, Yap YT, Danquah MK, Harun R. Thermochemical conversion of microalgal biomass for biofuel production. *Renew Sustain Energy Rev* 2015;49:990–9.
 - [16] Francisco EC, Neves DB, Jacob-Lopes E, Franco TT. Microalgae as feedstock for biodiesel production: carbon dioxide sequestration, lipid production and biofuel quality. *J Chem Technol Biotechnol* 2010;85(3):395–403.
 - [17] Borowitzka MA, Siva CJ. The taxonomy of the genus *Dunaliella* (Chlorophyta, Dunaliellales) with emphasis on the marine and halophilic species. *J Appl Phycol* 2007;19(5):567–90.
 - [18] Ertürk MD, Saçan MT. First toxicity data of chlorophenols on marine alga *Dunaliella tertiolecta*: correlation of marine algal toxicity with hydrophobicity and interspecies toxicity relationships. *Environ Toxicol Chem* 2012;31:1113–20.
 - [19] Okay O, Gaines A. Toxicity of 2,4-D acid to phytoplankton. *Water Resour* 1996;30:688–96.
 - [20] Ceylan S, Goldfarb J. Green tide to green fuels: TG–FTIR analysis and kinetic study of *Ulva prolifera* pyrolysis. *Energy Convers Manag* 2015;101:263–70.
 - [21] Marcilla A, Gómez-Siurana A, Gomis C, Chápuli E, Catalá M, Valdés F. Characterization of microalgal species through TGA/FTIR analysis: application to *nannochloropsis* sp. *Thermochim Acta* 2009;484:41–7.
 - [22] Hu Z, Chen Z, Li G, Chen X, Hu M, Laghari M, et al. Characteristics and kinetic studies of *Hydrilla verticillata* pyrolysis via thermogravimetric analysis. *Bioresour Technol* 2015;194:364–72.
 - [23] Xue J, Ceylan S, Goldfarb JL. Synergism among biomass building blocks? Evolved gas and kinetics analysis of starch and cellulose co-pyrolysis. *Thermochim Acta* 2015;618:36–47.
 - [24] Ceylan S, Kazan D. Pyrolysis kinetics and thermal characteristics of microalgae *Nannochloropsis oculata* and *Tetraselmis* Sp. *Bioresour Technol* 2015;187:1–5.
 - [25] Yang X, Zhang R, Fu J, Geng S, Cheng J, Sun Y. Pyrolysis kinetic and product analysis of different microalgal biomass by distributed activation energy model and pyrolysis–gas chromatography–mass spectrometry. *Bioresour Technol* 2014;163:335–42.
 - [26] Vyazovkin S, Burnham AK, Criado JM, Pérez-Maqueda LA, Popescu C, Sbirrazzuoli N. ICTAC kinetics committee recommendations for performing kinetic computations on thermal analysis data. *Thermochim Acta* 2011;520(1):1–19.
 - [27] Lakshmanan CC, White N. A new distributed activation energy model using Weibull distribution for the representation of complex kinetics. *Energy Fuels* 1994;8(6):1158–67.
 - [28] Burnham AK, Braun RL. Global kinetic analysis of complex materials. *Energy Fuels* 1999;13(1):1–22.
 - [29] Skrdla PJ. Crystallizations, solid-state phase transformations and dissolution behavior explained by dispersive kinetic models based on a Maxwell–Boltzmann distribution of activation energies: theory, applications, and practical limitations. *J Phys Chem A* 2009;113(33):9329–36.
 - [30] Miura K, Maki T. A simple method for estimating $f(E)$ and $k_0(E)$ in the distributed activation energy model. *Energy Fuels* 1998;12(5):864–9.
 - [31] Kebelmann K, Hornung A, Karsten U, Griffiths G. Intermediate pyrolysis and product identification by TGA and Py-GC/MS of green microalgae and their extracted protein and lipid components. *Biomass Bioenergy* 2013;49:38–48.
 - [32] Wang S, Jiang XM, Han XX, Wang H. Fusion characteristic study on seaweed biomass ash. *Energy Fuels* 2008;22(4):2229–35.
 - [33] OECD Guidelines for the Testing of Chemicals. Freshwater alga and cyanobacteria, growth inhibition test. March 23, 2006.
 - [34] Zainan N, Srivatsa S, Bhattacharya S. Catalytic pyrolysis of microalgae *Tetraselmis suecica* and characterization study using in situ synchrotron-based infrared microscopy. *Fuel* 2015;161:345–54.
 - [35] Maddi B, Viamajala S, Varanasi S. Comparative study of pyrolysis of algal biomass from natural lake blooms with lignocellulosic biomass. *Bioresour Technol* 2011;102(23):11018–26.
 - [36] Francavilla M, Kamaterou P, Intini S, Monteleone M, Zabaniotou A. Cascading microalgae biorefinery: fast pyrolysis of *Dunaliella tertiolecta* lipid extracted-residue. *Algal Res* 2015;11:184–93.
 - [37] Chen C, Ma X, Liu K. Thermogravimetric analysis of microalgae combustion under different oxygen supply concentrations. *Appl Energy* 2011;88(9):3189–96.
 - [38] Sydney E, Sturm W, Carvalho J, Thomaz-Soccol V, Larroche C, Pandey A. Potential carbon dioxide fixation by industrially important microalgae. *Bioresour Technol* 2010;101:5892–6.
 - [39] Lakaniemi A-M, Hulatt CJ, Thomas DN, Tuovinen OH, Puhakka JA. Biogenic hydrogen and methane production from *Chlorella vulgaris* and *Dunaliella tertiolecta* biomass. *Biotechnol Biofuels* 2011;4(34):1–12.
 - [40] Ali S, Razzak S, Hossain M. Apparent kinetics of high temperature oxidative decomposition of microalgal biomass. *Bioresour Technol* 2015;175:569–77.
 - [41] Bui H, Tran K, Chen W. Pyrolysis of microalgae residues – a kinetic study. *Bioresour Technol* 2016;199:362–6.
 - [42] Shuping Z, Yulong W, Mingde Y, Chun L, Junmao T. Pyrolysis characteristics and kinetics of the marine microalgae *Dunaliella tertiolecta* using thermogravimetric analyzer. *Bioresour Technol* 2010;101(1):359–65.
 - [43] Soria-Verdugo A, García-Hernando N, Garcia-Gutierrez LM, Ruiz-Rivas U. Analysis of biomass and sewage sludge devolatilization using the distributed activation energy model. *Energy Convers Manag* 2013;65:239–44.
 - [44] Yorulmaz SY, Atımtay AT. Investigation of combustion kinetics of treated and untreated waste wood samples with thermogravimetric analysis. *Fuel Process Technol* 2009;90(7):939–46.
 - [45] Goldfarb JL, Liu C. Impact of blend ratio on the co-firing of a commercial torrefied biomass and coal via analysis of oxidation kinetics. *Bioresour Technol* 2013;149:208–15.
 - [46] Sanchez-Silva L, López-González D, Garcia-Minguillan AM, Valverde JL. Pyrolysis, combustion and gasification characteristics of *Nannochloropsis gaditana* microalgae. *Bioresour Technol* 2013;130:321–31.
 - [47] Kim SS, Ly HV, Kim J, Lee EY, Woo HC. Pyrolysis of microalgae residual biomass derived from *Dunaliella tertiolecta* after lipid extraction and carbohydrate saccharification. *Chem Eng J* 2015;263:194–9.
 - [48] Kirtania K, Bhattacharya S. Pyrolysis kinetics and reactivity of algae–coal blends. *Biomass Bioenergy* 2013;55:291–8.
 - [49] Hui Z, Huaxiao Y, Mengmeng Z, Song Q. Pyrolysis characteristics and kinetics of macroalgae biomass using thermogravimetric analyzer. *Proc World Acad Sci Eng Technol* 2010;65:1161–6.
 - [50] Li D, Chen L, Zhao J, Zhang X, Wang Q, Wang H, et al. Evaluation of the pyrolytic and kinetic characteristics of *Enteromorpha prolifera* as a source of renewable bio-fuel from the Yellow Sea of China. *Chem Eng Res Des* 2010;88(5):647–52.